Measurements of the Primary Bjerknes Force in a Cavitating Ultrasonic Field

By
Mason Smith

A thesis submitted to the faculty of The University of Mississippi in partial fulfillment of the requirements of the Sally McDonnell Barksdale Honors College.

Oxford
May 2019

Approved by

_____
Advisor: Dr. Joel Mobley

_____
Reader: Dr. Cecille Labuda

_____
Reader: Dr. Joseph Gladden

DEDICATION

I would like to dedicate this work to my parents, Billy and Rochelle. I am forever grateful for the amount of love and care that they have invested in me.

ACKNOWLEGEMENTS

I would first like to thank Dr. Joel Mobley. He has been an excellent mentor and research advisor. If it were not for Dr. Mobley, then I would never have learned about the Basic Acoustic Summer School (BASS) program. It was during the BASS program that I participated in research at the National Center for Physical Acoustics (NCPA). I am very thankful for Dr. Mobley allowing me the opportunity to work with him and am thankful for his patience in completing this thesis.

I would next like to thank my readers. Dr. Labuda and Dr. Gladden very kindly agreed to be readers for this work, so if it were not for them, I would not have been able to complete this thesis.

My next thank you is for Randa Baioni. She has been my best friend since we first met in Honors 101. She has helped me through tough times and continues to still support me. I am very grateful for our friendship.

To my father, mother, and brothers, thank you for believing in me. Thank you for your love and support of me.

And finally, I would like to thank the Sally McDonnell Barksdale Honors College for encouraging me to complete this thesis. I am very thankful for this opportunity to share my research.

ABSTRACT

Cavitation is the result when there are rapid changes in pressure in a liquid. These vapor-filled cavities can occur when ultrasound propagates through water at sufficient power. The volumes of these cavities can pulsate and can even couple with the radiation pressure from the ultrasound. The result is a translational force on the bubbles. This translational force on the bubble is called the primary Bjerknes force. The secondary Bjerknes force is the result of two pulsating cavities, but this force is ignored since the buoyant force and the primary Bjerknes force are the dominant forces. Immediately before a bubble begins to rise, the net force on the bubble is equal to zero. Therefore, the primary Bjerknes force and the buoyant force are equal. The primary Bjerknes force can be indirectly measured by measuring the diameter (and thus the volume) of a bubble immediately before it rises. Diameters of bubbles were measured using a video camcorder and an open-source program called ImageJ. Three sets of data were taken. Each set of data includes four critical bubbles. The primary Bjerknes force ranges from 0.15 μN to 0.41 μN. Recent research and future work are discussed.

TABLE OF CONTENTS

LIST OF FIGURES AND TABLES

1 INTRODUCTION

The physical phenomenon of sound is one that most people are familiar with. The branch of physics that is concerned with the propagation of mechanical waves through solids, liquids, and gases is known as acoustics. The study of acoustics dates back to the 6th century BCE when Pythagoras mathematically described the properties of stringed musical instruments (Karamanides, 2006). As time progressed and the study of naturally-occurring phenomena was unified in what we now know as the science of physics, mechanical waves became better understood and described in mathematical terms (Berg, 2018). Sound can be classified according to frequency. These classifications are infrasound (sound with frequencies below which humans can hear), sound (sounds with frequencies which humans can hear), and ultrasound (sound with frequencies above which humans can hear). While the study of infrasound and sound cover a variety of subjects, the study of ultrasound reveals a wide variety of applications and unusual phenomena.

Ultrasound was first encountered in the 18th century by Italian scientist Lazzaro Spallanzani during his study of echolocation in bats (Bates, 2011). Ultrasound was first produced by humans when Sir Francis Galton created what is now known as a Galton whistle (History of Ultrasound | Timeline since 1794, 2014). Ultrasound has many useful applications. One of these applications is non-destructive testing (NDT) which was first proposed in 1929 by Russian scientist

Sergei Sokolov (A Brief History of Non-Destructive Testing, 2014). The use of ultrasound in modern medicine is made possible by the use of ultrasonic transducers. These transducers make use of the piezoelectric effect, which was discovered in 1880 by French physicists Pierre and Paul-Jacques Curie (*Piezoelectricity*, 2018). The study of the primary Bjerknes force is one that is motivated by innovations in modern medicine for drug delivery. One proposed way of delivering drugs to particular sites within a body is to use polymer-coated microbubbles (Memoli et al, 2018). Therefore, it is important to know how the primary Bjerknes force interacts with microbubbles.

2 THE PROPAGATION OF ULTRASOUND THROUGH WATER

When ultrasound of sufficient power propagates through water, it can create cavitation bubbles. These are gas-filled cavities that are formed during the negative pressure phase of the acoustic cycle. A small air pocket on a piece of particulate matter, which is itself too small to be seen, grows during the negative pressure phase. As it grows, gases dissolved in the water are drawn into the bubble, allowing it to grow to a size large enough to be visualized. Acoustic cavitation is a high power phenomenon. At low powers, ultrasound will propagate through the water as a normal wave without changing the structure (e.g., introduction cavitation bubbles) of the medium. Once the bubbles are generated, they can be trapped by the gradient in the ultrasonic pressure field.

3 THE PRIMARY BJERKNES FORCE

3.1 THEORY OF THE PRIMARY BJERKNES FORCE

It was in 1906 when Norwegian physicist Vilhelm Bjerknes (Figure 1) published *Fields of Force*. In *Fields of Force*, Bjerknes begins by describing electric and magnetic fields. He then extends this treatment of electric and magnetic fields to fields – specifically those in hydrodynamics – that have analogous properties. It was in this way that Bjerknes was able to mathematically derive the translational force on bubbles in an acoustic field.

Gases are dissolved in liquids. These gases in water can be excited and thus can increase in volume. When these gases increase in volume, gas-filled bubbles form. Gas-filled bubbles that are subject to an acoustic pressure field undergo volume oscillations. These volume oscillations can couple with a non-zero acoustic pressure gradient. The result is a translational force known as the primary Bjerknes force. The primary Bjerknes force is equal to the negative product of the time-varying volume of a bubble and the pressure gradient. If this product varies with time, then the time average is taken.

$$\vec{F} = -\langle V(t)\nabla P(r,t)\rangle$$

This translational force was first formulated by Bjerknes (1906) but was later described by Blake (1949). As ultrasound travels through water, dissolved gases increase in volume and become gas-filled bubbles. If these gas-filled bubbles

Figure 1 Picture of Vilhelm Bjerknes. Bjerknes (1862-1951) was a Norwegian physicist who helped establish the modern field of meteorology. It is after Bjerknes for which the primary Bjerknes force is named. https://snl.no/Vilhelm_Bjerknes

occur at pressure antinodes, they migrate away. These gas-filled bubbles become trapped by pressure gradients and begin to coalesce. The forces on these bubbles are the buoyant force, the primary Bjerknes force, and the secondary Bjerknes force. The secondary Bjerknes force is a force between two pulsating bubbles and is not considered in this work because we are assuming that the the primary Bjerknes force has the most influence on the trapping of a bubble in the field.

3.2 EQUATION OF THE PRIMARY BJERKNES FORCE

The primary Bjerknes force is given by

$$\vec{F} = -\langle V(t)\nabla P(r,t)\rangle$$

The time-varying volume $V(t)$ can be described in terms of a time-varying radius given by

$$R\ddot{R} + \frac{3}{2}\dot{R}^2 = \frac{1}{\rho}\left[\left(P_0 + \frac{2\sigma}{R_0} - P_v\right)\left(\frac{R_0}{R}\right)^{3\kappa} - \frac{2\sigma}{R} - \frac{4\mu\dot{R}}{R} - P_0 - P(t)\right]$$

where R_0 is the equilibrium radius of a bubble, P_0 is the hydrostatic pressure, P_v is the vapor pressure inside the bubble, κ is the polytropic index of the gas, $P(t)$ is the time-varying pressure, and ρ, σ, and μ are the liquid density, the surface tension, and the viscosity of the liquid, respectively (Leighton, 1989). This equation is known as the Rayleigh-Plesset equation and is derived from the Navier-Stokes equation under the assumption that the bubbles are spherically symmetric. When the acoustic field is continuous, the magnitude of the primary Bjerknes force can be written as

$$F = \alpha\frac{P_A \pi f V_0}{c_w}$$

where α is a constant, P_A is the pressure amplitude, f is the frequency, V_0 is the equilibrium volume of a bubble, and c_w is the speed of sound in water.

4 INITIAL RESEARCH OF THE PRIMARY BJERKNES FORCE

4.1 EXPERIMENTAL SETUP

The setup for measuring the primary Bjerknes force includes both optical and acoustic instruments. The purpose of the measurement system is to provide estimates of the primary Bjerknes force. The approach is known as the scattered light method and was the method used in this work to determine the force. This setup allows for the direct measurement of the volumes of bubbles. From the volumes of bubbles, buoyant forces can be calculated. It is from the buoyant forces that the primary Bjerknes force on bubbles can be calculated. In this method, light is scattered off of the bubbles in a forward scattering manner. When light is forward scattered, the bubbles are only visible from a particular direction (i.e., from the direction in which the light is traveling). This is analogous to seeing dust in a room in a sunbeam. The sunlight that is incident of the dust scatters forward in a way that makes the dust visible, while in the backward direction the dust is not visible. Figure 2 is a schematic diagram of the setup for the scattered light method. Figure 3 is a picture of the setup. An ultrasonic transducer is immersed in water and is connected to a radiofrequency (RF) generator. The RF generator provides a sinusoidal voltage to the piezoelectric crystal in the transducer and allows for adjustments of the frequency and power applied to the transducer. Figure 4 is a picture of the transducer and the metal plate. The red block is used to raise the reflector so it is

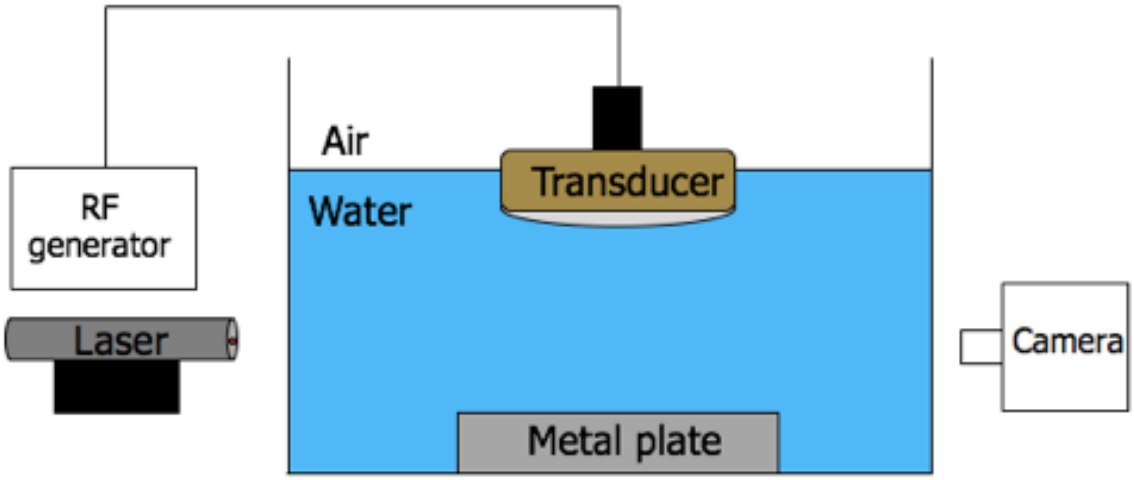

Figure 2 Schematic diagram of the setup. This figure illustrates the setup for measuring the primary Bjerknes force. The transducer is powered by the radiofrequency (RF) generator. As ultrasound travels through the water creating cavitation, it strikes the metal plate, traveling back to the transducer. The result is a standing wave which influences the cavitation created by the ultrasound. Data is recorded using the camera. The laser allows for planes of the cavitation to be illuminated.

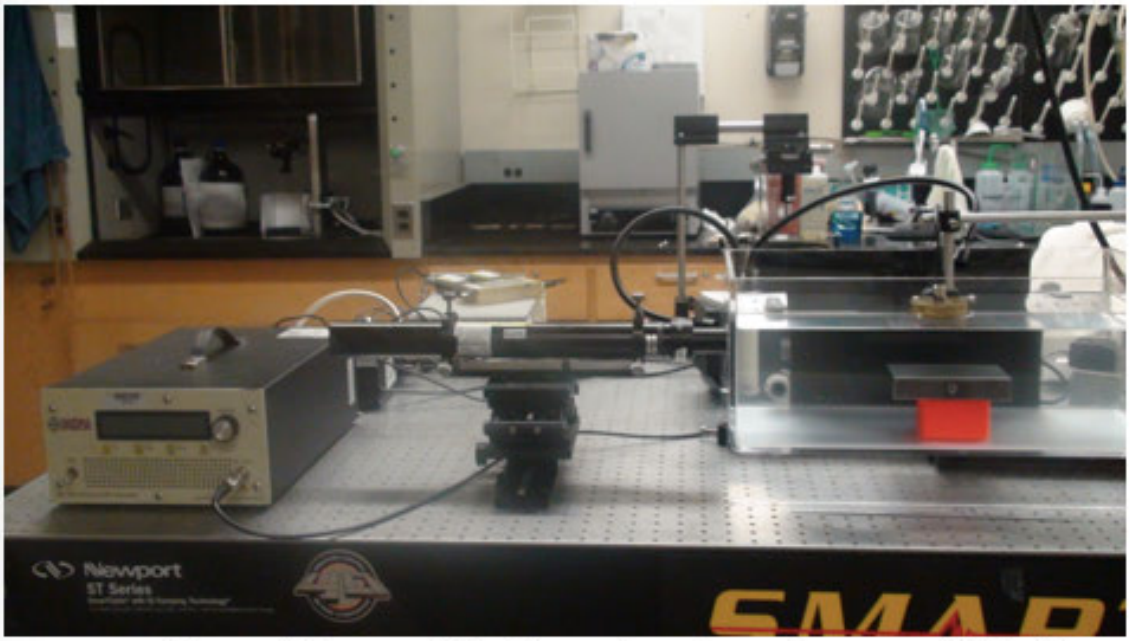

Figure 3 Picture of the setup. This picture shows the equipment used. The video camcorder is not pictured but is typically placed in front of the tank.

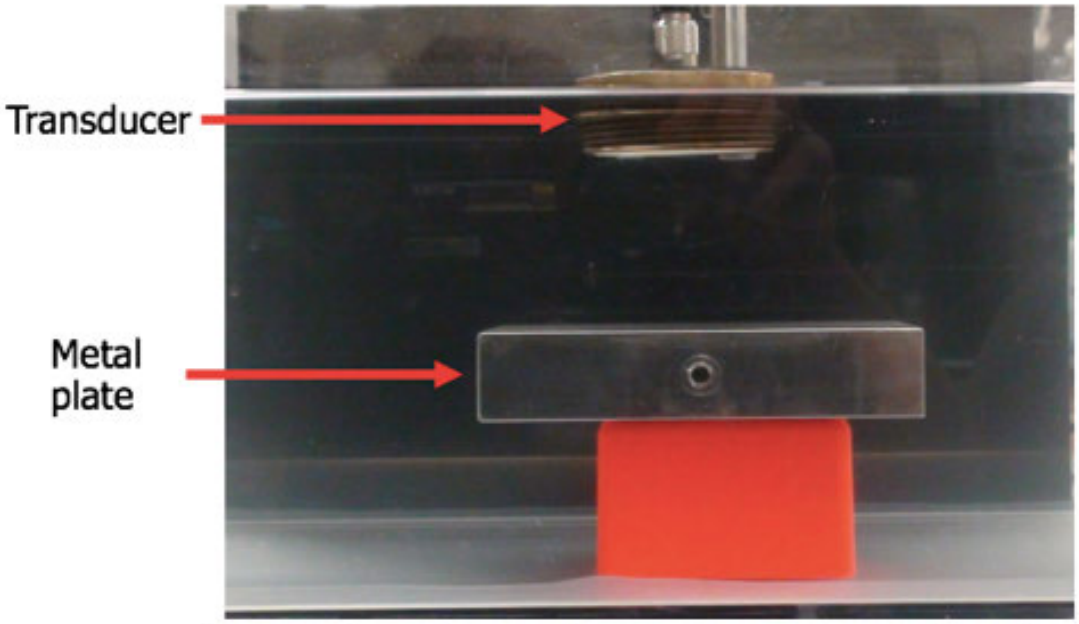

Figure 4 Close-up of transducer and reflector. This picture shows the reflector sitting atop a red block. When using the laser, it was difficult to adjust the height of the laser. The red block thus allowed for the metal plate to be closer to the transducer which helps to track the position of the laser slice.

closer to the transducer. As ultrasound propagates through the water, it strikes the reflector and travels back towards the transducer. Ultrasound in a liquid is a longitudinal wave, and the interference of the counter-propagating waves creates a standing wave. The waves generate cavitation bubbles which are trapped in the nodes of the standing wave. Conversely, the antinodes of the standing wave are places from which bubbles move. Figure 5 is a picture that demonstrates bubbles that are trapped in nodes. These nodes are places where pressure is zero, and conversely, the antinodes are places where the pressure oscillates with maximum amplitude. The spacing between the bubbles is equal to one-half of the wavelength of the ultrasound.

The speed of sound in water c can be calculated by using a fifth-order polynomial that was fitted to experimental data points (Marczak, 1997). This fifth-order polynomial is

$$c = \sum_{n=0}^{5} a_n T^n$$

where a_i are coefficients and where T is temperature in °C. Plugging the coefficients into this sum,

$$\begin{aligned} c = {} & (1.402385\times10^{3}) + (5.038813\times10^{-3})T + (-5.799136\times10^{-5})T^2 \\ & + (3.287156\times10^{-7})T^3 + (-1.398845\times10^{-9})T^4 \\ & + (2.787860\times10^{-12})T^5 \end{aligned}$$

The temperature of the water was 21°C in Figure 5. This means that $c \approx 1485$ m/s. The frequency f of the ultrasonic transducer was 1.2 MHz. Therefore, the wavelength λ of the ultrasound was

$$\lambda = \frac{c}{f}$$

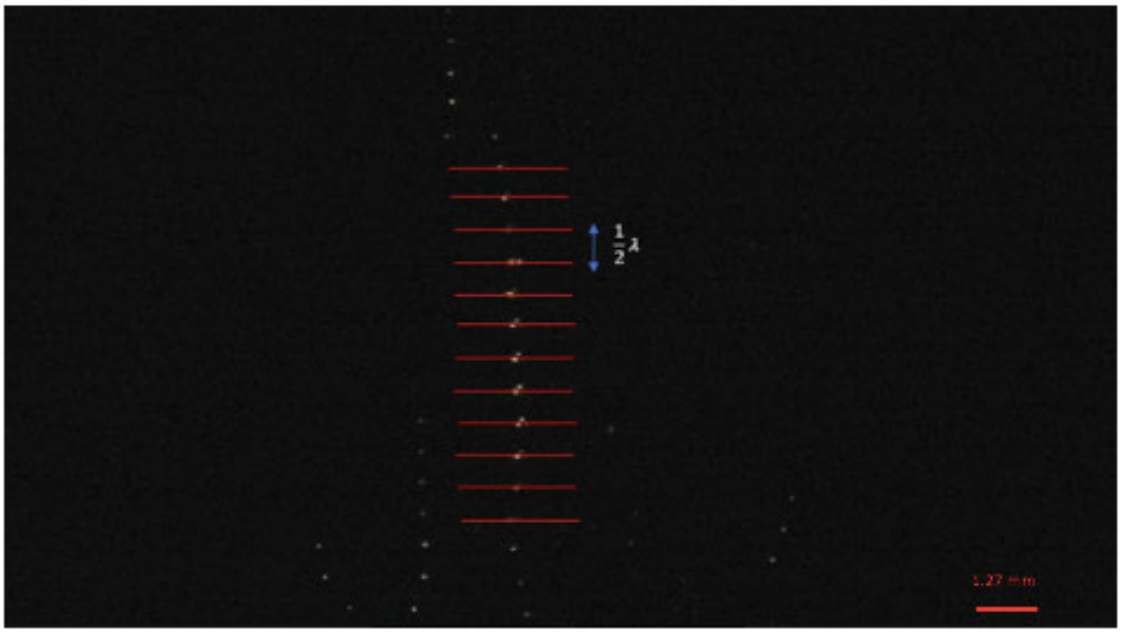

Figure 5 Line of bubbles. This pictures shows the bubbles evenly spaced. Each bubble is located in a pressure node. The lines that cross through the bubbles serve to illustrate the spacing between the bubbles.

$$\lambda = \frac{1485\ \mathrm{m \cdot s^{-1}}}{1.2\times10^{-6}\ \mathrm{s^{-1}}}$$

$$\lambda = 1.24\ \mathrm{mm}$$

The wavelength was measured to be 1.27 mm, a percent difference of only 2% relative to the theoretical value.

4.2 METHODS

As was mentioned in the previous section, the cavitation is captured on a video camcorder that is placed in front of the tank and adjusted so that the bubbles are clearly visualized. Figure 6 is an image taken of the cavitation. At first glance it may not appear that there is much regularity in the cavitation field, but there exist repeating structures. This can be seen in Figures 7 and 8. An examples of a structure that repeats multiple times throughout the cavitation field is the side lobe.

One of the goals of this research was to classify bubbles based on their sizes and how they behave. The bubbles that are examined first are those that we classify as small. In this method, it was not possible to determine the forces on these bubbles because they remain trapped throughout the experiment, so these bubbles are not mentioned in Table 1. Nevertheless, these smaller bubbles are important and therefore are described here. They have a radius of approximately 0.05 mm. The bubbles that are most prominent among them are the ones along strands. These bubbles are stationary relative to the larger bubble types. Their motion consists mostly of small displacements from what can be considered their equilibrium positions. As a result, they remain fixed in the ultrasound field. Medium, or transitional, bubbles occur where stationary bubbles coalesce. They begin to have large displacements from what can be considered their equilibrium positions. Large,

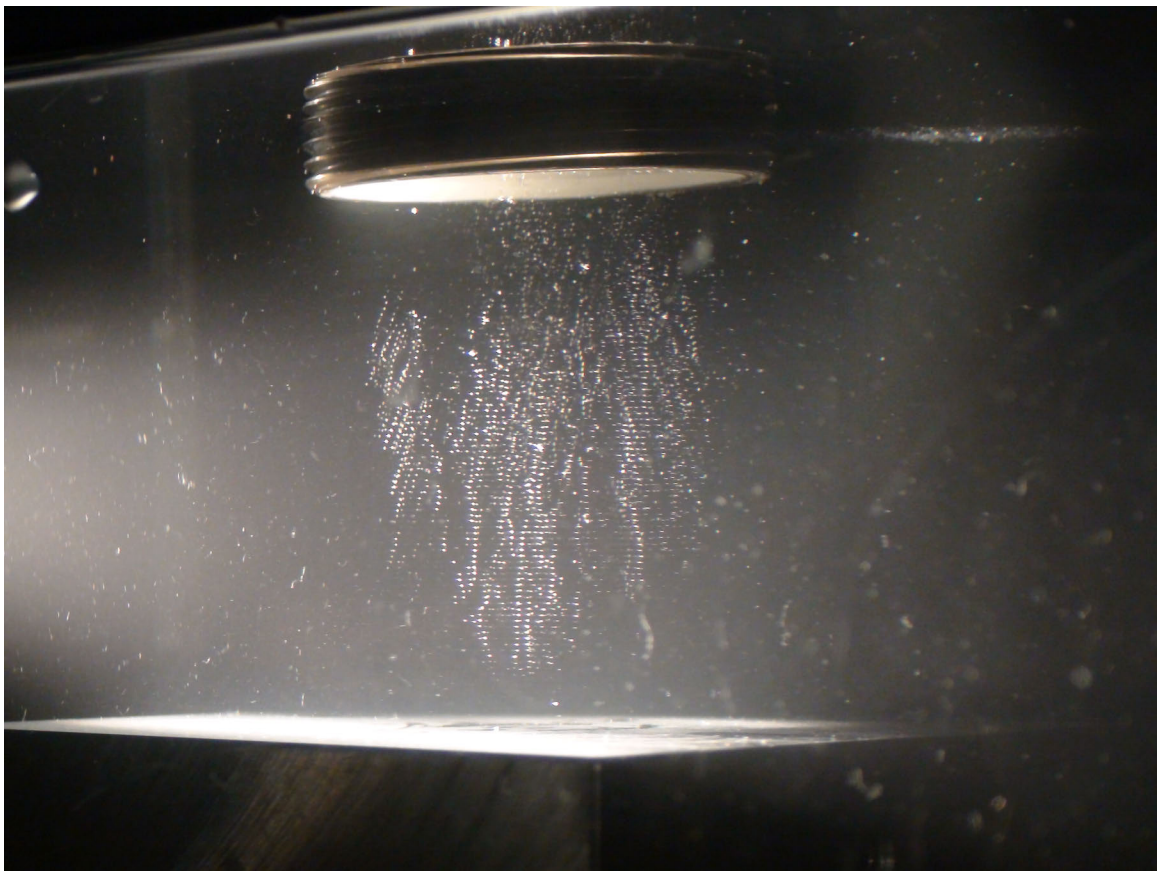

Figure 6 Field of cavitation. This figure shows the “cloud” of cavitation.

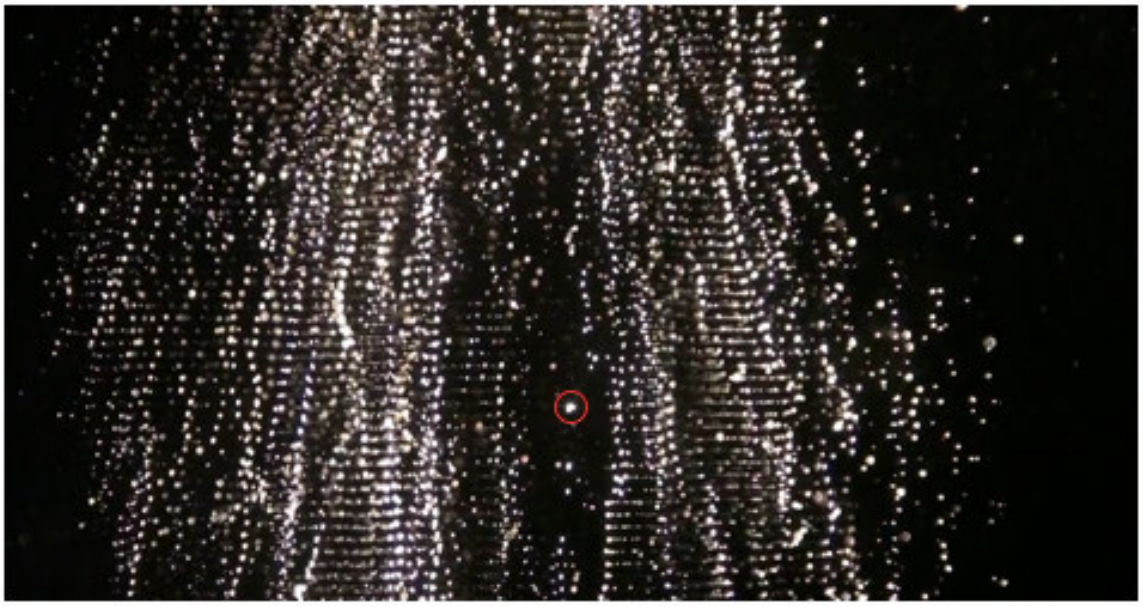

Figure 7 Close-up of cavitation. The bubble that is enclosed in a red circle is a critical bubble. This figure was taken immediately before the bubble began to rise. In addition to this critical bubble are a large number of other bubbles, all undergoing some sort of activity.

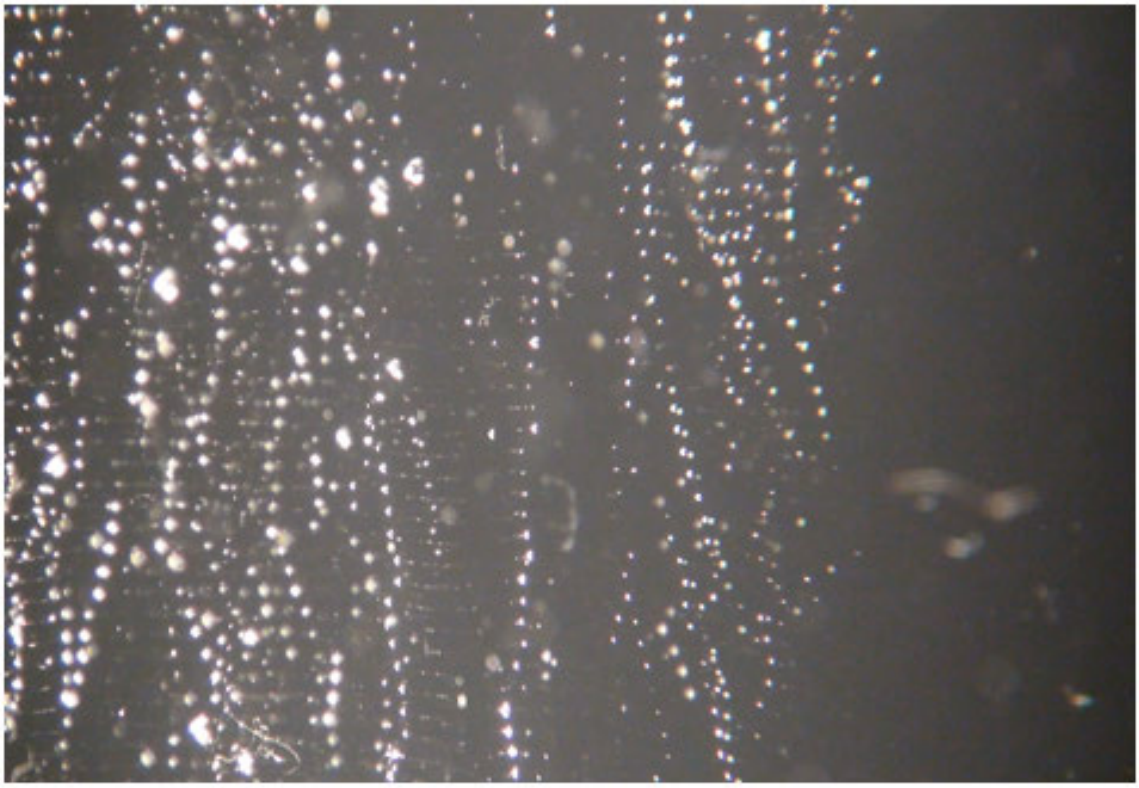

Figure 8 Close-up to illustrate structure. There are two prominent structures which exist in this figure. The first type of prominent structures are the strands of bubbles, and the second type of prominent structures are the side lobes.

or critical, bubbles are of primary interest. Critical bubbles may be the same size or larger than transitional bubbles. Before critical bubbles begin to rise, their ranges of motion are quite large. A critical bubble will begin to rise once its buoyant force exceeds the primary Bjerknes force.

To estimate the magnitude of the primary Bjerknes force, the volume of the bubble needs to be measured. Developed by the National Institutes of Health (NIH) in 1997, ImageJ (https://imagej.nih.gov/ij/download.html) is an open-source program that was used to measure the diameter of bubbles. ImageJ can help facilitate precise measurements. However, the precision of measurements is only as good as the scale set by a user.

There were two main issues encountered when identifying and tracking critical bubbles. The first issue was the number of bubbles in the cloud of cavitation. There exist a large number of bubbles in a cloud. Using water that has been distilled and degassed helps reduce the amount of cavitation but not by a significant amount. The second issue was identifying the location of the bubble within the cloud. Data is recorded with a video camcorder, and it is not possible to measure the depth of a critical bubble from a two-dimensional image. A solution to these two problems is to illuminate a plane of the field of cavitation. This is analogous to computed tomography (CT), an invaluable diagnostic imaging tool that allows doctors to view "slices" of patients' bodies. The concept of illuminating a plane in the cloud of cavitation is illustrated in Figure 9. Laser light is collimated and is passed through a thin aperture. This is shown in Figure 10. The result is a plane-like beam of collimated laser light that is incident on the field of cavitation. Figure 11 shows how the

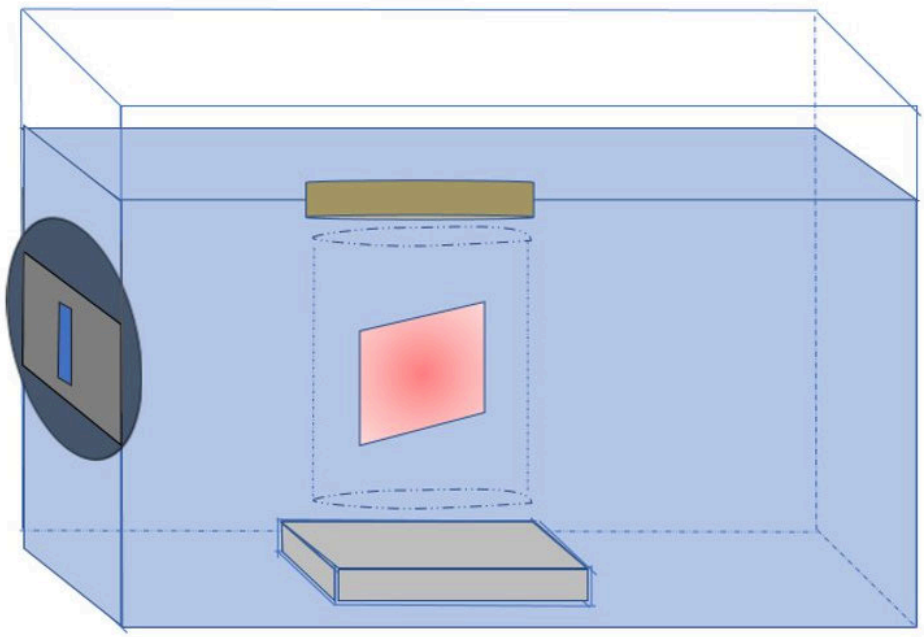

Figure 9 Schematic setup of laser light. This figure illustrates the concept for illuminating a plane of cavitation with laser light.

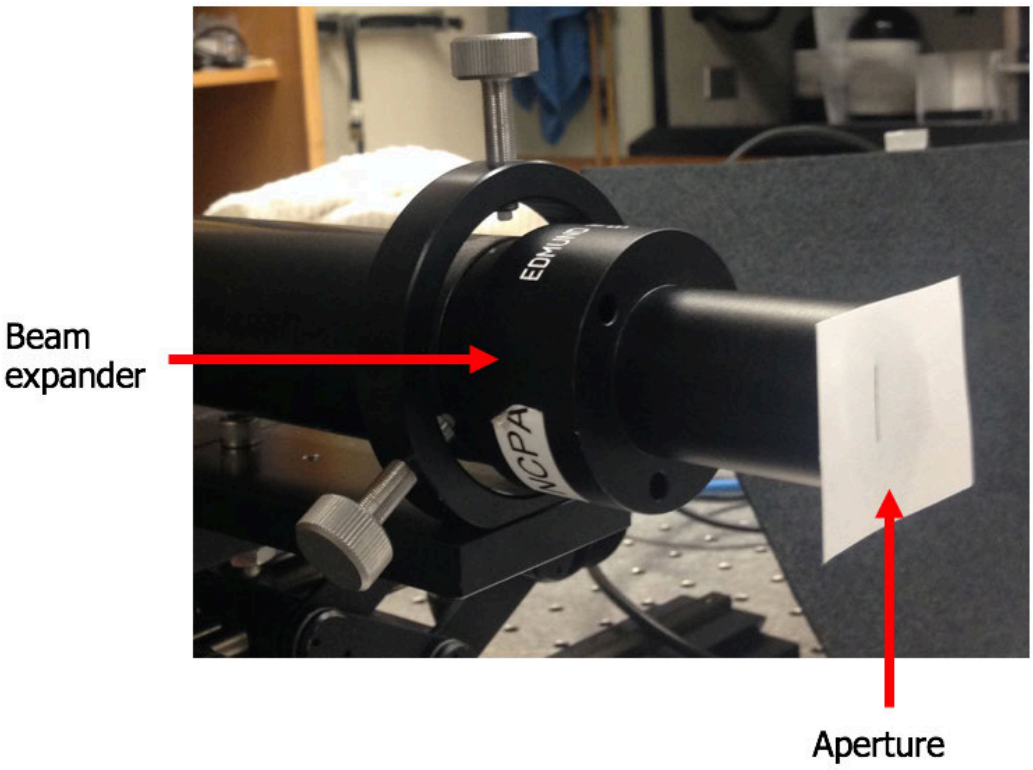

Figure 10 Laser with collimator and aperture. Attached to this laser is a beam expander and an aperture. The beam expander widens the diameters of the the laser light and forms it into a column, and the aperture restricts the laser light to a plane that will illuminate a slice of the cavitation cloud.

cavitation field appears whenever a plane of interest is illuminated. This method allows one to focus on a single plane rather than the entire cavitation field. The advantage is that we can focus attention on a group of bubbles rather than an entire cavitation cloud, as visualized in Figure 12. This makes it easier to identify the positions of critical bubbles.

4.3 DATA AND RESULTS

Data were collected in three sets. Each set of data consists of four measurements. The data includes the power and the frequency settings on the RF generator and the approximate location of the critical bubbles. Table 2 lists some of the data. These approximate locations are identified from the front of the setup (i.e., from where the video camcorder was placed). The reason that the power and frequency were varied was so that the reflected power from the generator to the transducer was at a minimum. In other words, the power and frequency were varied so that the maximum amount of power provided was used by the transducer. Figures 13 through 15 list the average critical diameters, the average critical volumes, and the average critical forces, respectively, for each data set. The diameter of each bubble is measured in each set. The critical diameters are then averaged. In a similar way, the critical volumes and the critical forces are calculated for each bubble in each set. Table 3 summarizes the information presented in these figures.

Figure 11 Illuminating a plane of cavitation. The top picture is a reference picture for the bottom picture. The bottom picture shows a plane of bubbles that is illuminated with laser light.

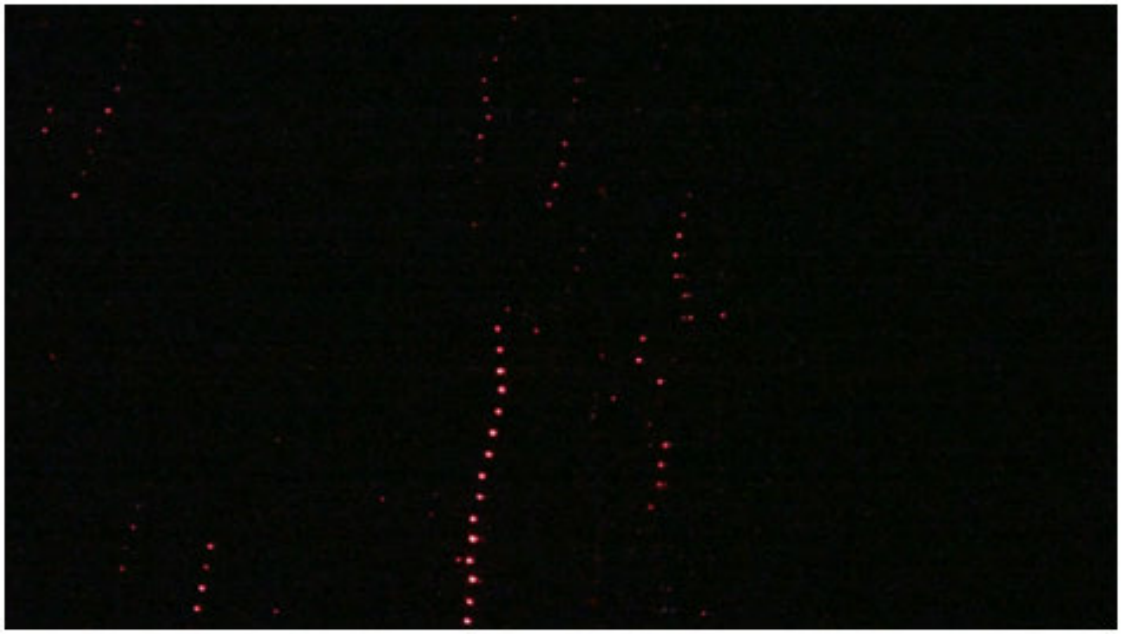

Figure 12 Close-up of a plane of bubbles. This figure shows strands of bubbles illuminated by laser light.

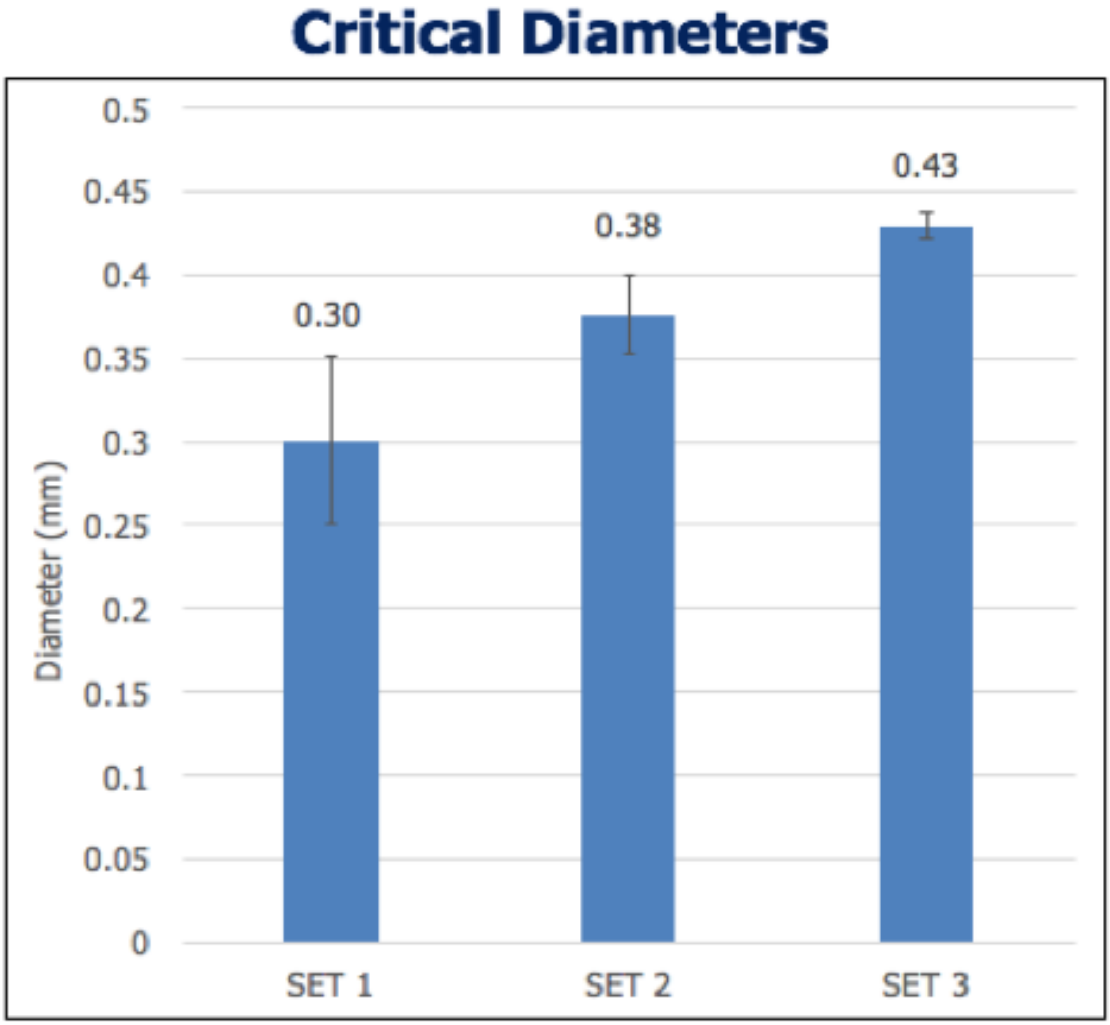

Figure 13 This graph shows the average critical diameters for the three sets of data (N=4).

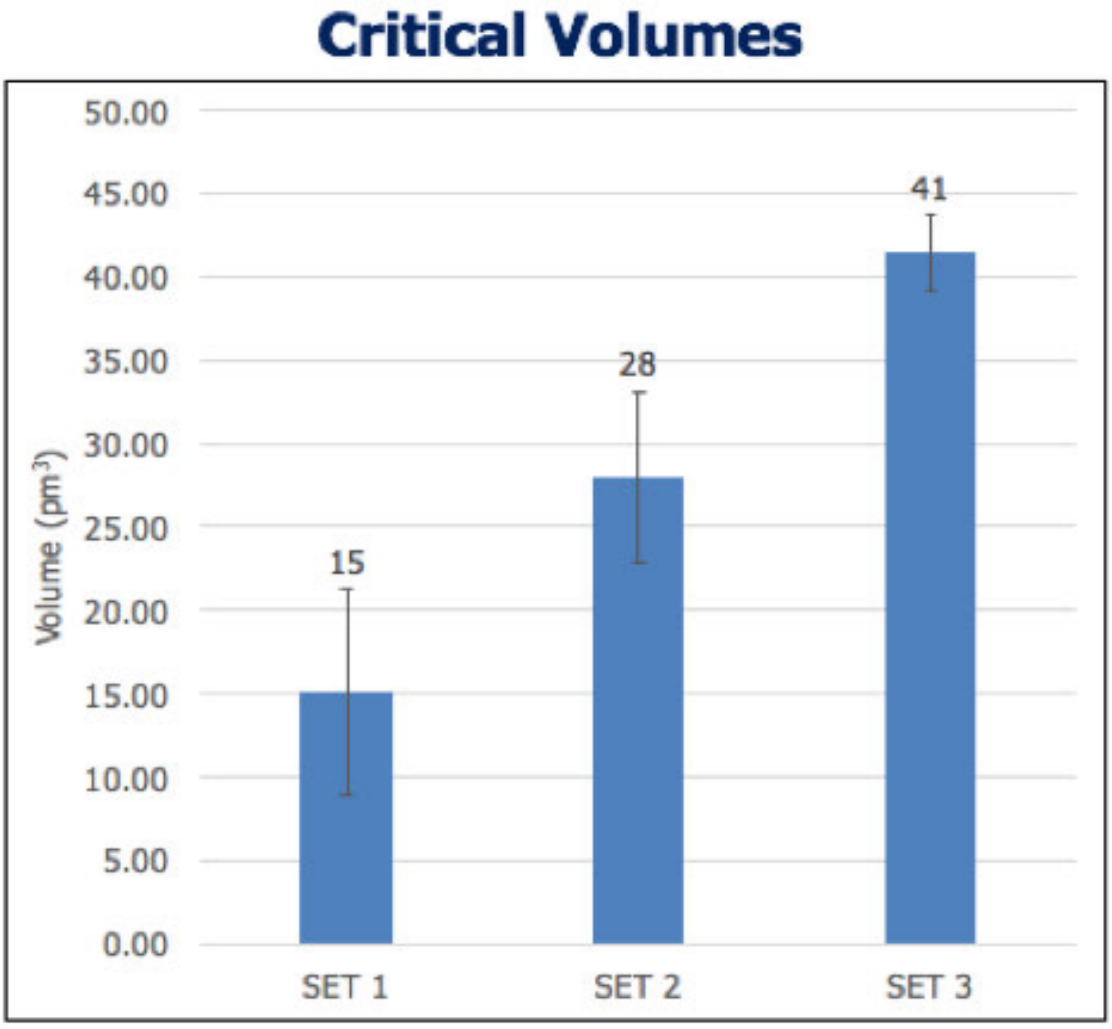

Figure 14 This graph shows the average critical volumes for the three sets of data (N=4).

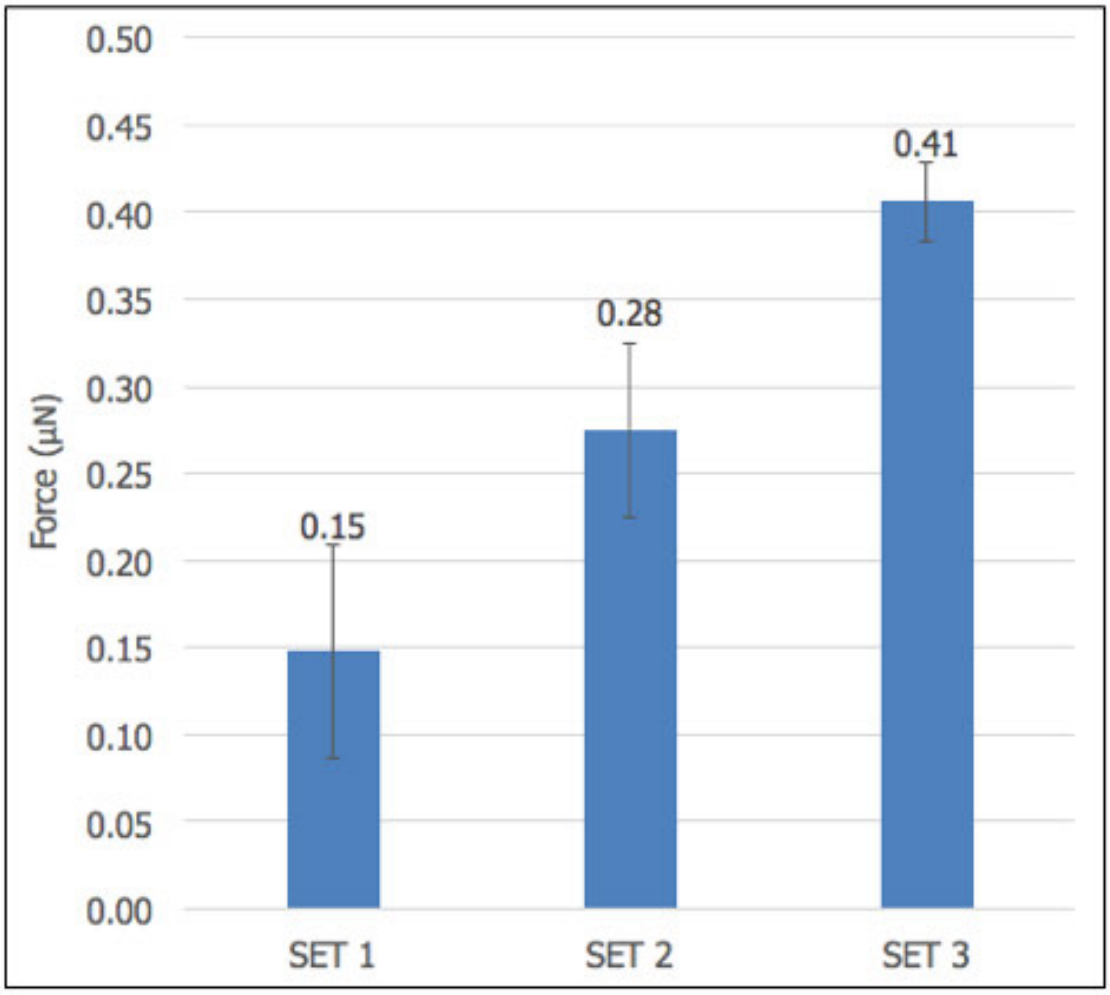

Figure 15 This figure shows the average critical force for the three sets of data (N=4).

Table 1: Classification of Bubbles	
	Motion
Small/stationary	Slightly move around and are arranged in strands
Medium/transitional	Move around more than stationary bubbles but do not rise
Large/critical	Move around just as much as transitional bubbles and are able to rise

Table 1 This table summarizes the classification of bubbles.

Table 2: Some Data for Sets			
	Power (W)	Frequency (MHz)	Approximate Location
Set 1	10	1.12	Middle of field between the transducer and the reflector
Set 2	15	1.10	Middle of the field between the transducer and the reflector
Set 3	20	1.00	Middle of the field to the right of the transducer

Table 2 This table lists some data for the sets of bubbles.

Table 3: Summary of Measurements			
	Average Critical Diameter (mm)	Average Critical Volume (pm^3)	Average Critical Forces (μN)
Set 1	0.30(5)	15(6)	0.15(6)
Set 2	0.38(3)	28(5)	0.28(5)
Set 3	0.43(1)	41(2)	0.41(2)

Table 3 This table lists the average critical diameters, average critical volumes, and average critical forces for the sets. The numbers in parentheses indicate the uncertainty in the last digit.

5 RECENT RESEARCH OF THE PRIMARY BJERKNES FORCE

5.1 IMPROVEMENT OF METHODS

The initial measurements of the primary Bjerknes force ranged from 0.15 μN to 0.41 μN. As mentioned before, these measurements should really be referred to as estimates. A force that is comparable to the primary Bjerknes force is the weight (on Earth) of a single grain of sand.

One problem with the scattered light method was the uncertainty of the diameter of the bubbles. In addition to not knowing the exact diameters of bubbles, the exact location of the bubbles remained unknown. Again, the locations of the bubbles were approximate and were based on their positions relative to the transducer. Fortunately, these two problems can be resolved.

The first of these problems arises from the scattered light. When light scatters from a bubble, it may refract several times inside a bubble before it exits. This makes the bubble appear bright. The result is a bubble that is not well defined. Instead of scattering light from the bubbles, it was decided that it would be better to have light be diffused and to be behind the bubbles. This allows the edges of the bubbles to be well defined, as shown in Figure 16.

A solution to the second problem mentioned is to simply use a second camera that is 90° from the first. This allows for the determination of the positions of critical bubbles in three dimensions.

Figure 16 Bubbles in diffuse light. This figure shows how well defined the bubbles are whenever light is diffused behind the bubbles.

5.2 RECENT DATA AND RESULTS

Results from the improved setup agree with results from the initial setup. Figure 17 shows a critical bubble (indicated by the arrow) that has a diameter of 1.04 mm. Its position, as measured from the origin *O* of the axis, is also given and is in units of mm. The primary Bjerknes force on this critical bubble was calculated to be 5.8 μN. Figure 18 shows a side-by-side comparison of a critical bubble that is viewed from different angles. The improvement of methods for measuring the primary Bjerknes force is part of an on-going work to be reported in the future.

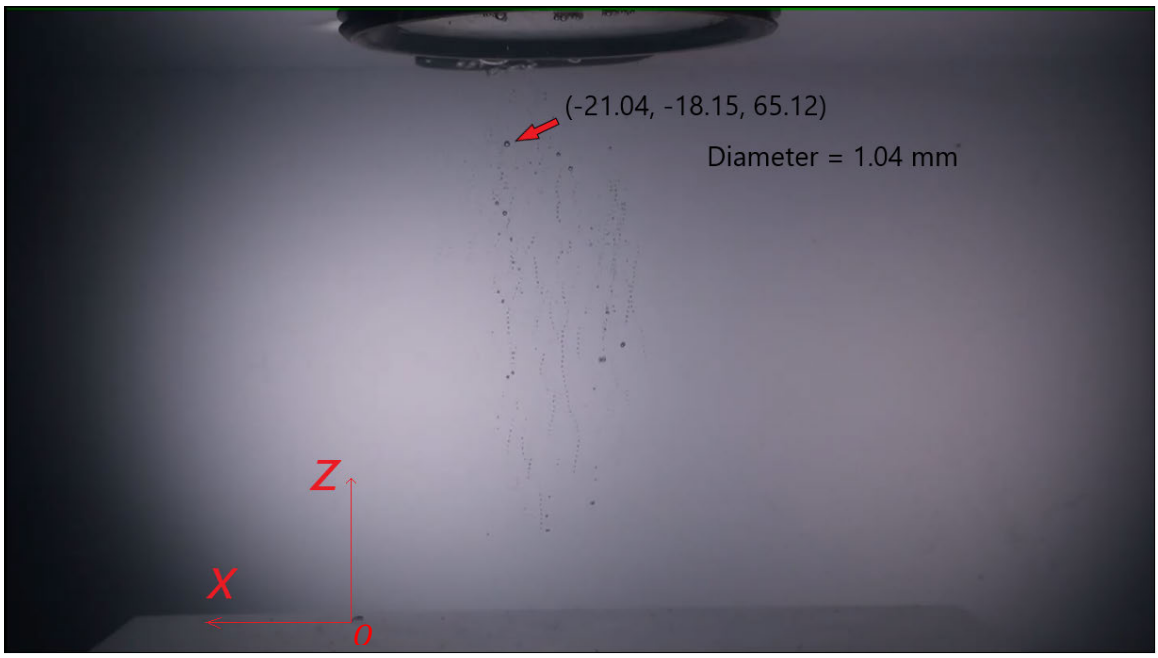

Figure 17 Recent measurement. This is Figure 13 but includes a measurement that offers a more precise determination of the diameter and position of the bubble than is offered by the scattered light method.

Figure 18 Side-by-side comparison. The bubbles that are encircled in red are the same bubbles. The picture on the left is taken from the front of the tank, and the picture on the right is taken from the side of tank.

6 CONCLUSIONS

Measuring the primary Bjerknes forces on bubbles is possible by first measuring the diameters of bubbles. Once the diameters of bubbles are known, the volumes of the bubbles can be calculated, thus leading to the buoyant forces. These buoyant forces are equal in magnitude to the primary Bjerknes forces immediately before the bubbles begin to rise. The primary Bjerknes forces ranged from 0.15 μN to 0.48 μN. The initial measurements of the primary Bjerknes force were based on the scattered light method. This method will be refined in future work by using diffuse light instead of scattered light. In addition to the diffuse light, a second camera will be used so that the location of the bubbles in three dimensions can be measured.

7 FUTURE WORK

Measurements of the primary Bjerknes force have been established but do need to be refined. One goal of future work is to improve the quality of the images so that the diameters of the bubbles can be better determined. In addition to better measurements of the diameters of bubbles, more sets of data should be recorded. Each set of data should vary in power and frequency so that trends can be identified. Also, measurements of the primary Bjerknes force should be compared to predictions. A hydrophone scan of the acoustic pressure is shown in Figure 19. These predictions will compare the radiation pressure measured in a location to the radiation pressure predicted by a model. It would be advantageous to use code to automate the measuring of critical bubbles and their locations relative to an origin and to track the motion of critical bubbles.

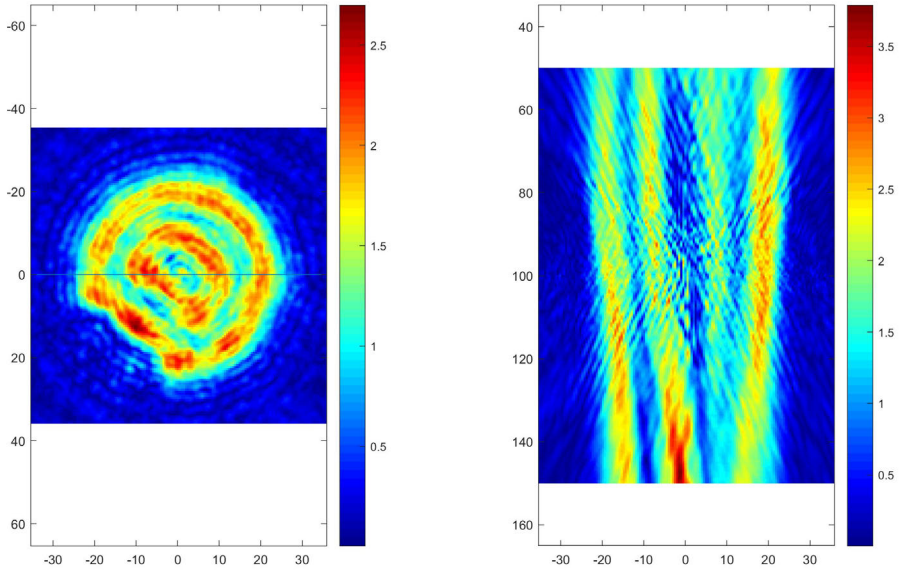

Figure 19 Hydrophone scan of transducer. These graphs show the magnitude of the acoustic pressure as a function of distance. The picture on the left shows the acoustic pressure as viewed looking directly up at the face of the transducer at a distance of approximately 7 cm. The picture of the right is a side-view of the magnitude of the acoustic pressure.

REFERENCES

Bates, M. (2011). Discovering sonar in bats, American Association for the Advancement of Science, Available: https://www.aaas.org/discovering-sonar-bats, (date last viewed: 01-May-19). Retrieved May 1, 2019, from https://www.aaas.org/discovering-sonar-bats

A Brief History of Non-Destructive Testing, (2014). A Brief History of Non-Destructive Testing - Non-Destructive Testing (NDT) Blog, Available: http://tspndt.com/non-destructive-testing-industrial-supplies-blog/a-brief-history-of-non-destructive-testing, (date last viewed: 01-May-19). Retrieved May 1, 2019, from http://tspndt.com/non-destructive-testing-industrial-supplies-blog/a-brief-history-of-non-destructive-testing

Berg, R. E. (2018). Acoustics, Encyclopædia Britannica, Available: https://www.britannica.com/science/acoustics/Modern-advances, (date last viewed: 01-May-19). Retrieved May 1, 2019, from https://www.britannica.com/science/acoustics/Modern-advances

Blake, F. G., Jr. (1949). "Bjerknes Forces in Stationary Sound Fields," The Journal of the Acoustical Society of America, 21, 551–551.

History of Ultrasound | Timeline since 1794, (2014). Ultrasound Technician Schools, Available: http://ultrasoundschoolsguide.com/history-of-ultrasound/, (date last viewed: 01-May-19). Retrieved May 1, 2019, from http://ultrasoundschoolsguide.com/history-of-ultrasound/

Karamanides, D. (2006). Pythagoras: pioneering mathematician and musical theorist of Ancient Greece, Rosen Central, New York

Leighton, T. G., Walton, A. J., and Pickworth, M. J. W. (1990). "Primary Bjerknes forces," European Journal of Physics, 11, 47–50.

Marczak, W. (1997). "Water as a standard in the measurements of speed of sound in liquids," The Journal of the Acoustical Society of America, 102, 2776–2779.

Memoli, G.; Baxter, K.O.; Jones, H.G.; Mingard, K.P.; Zeqiri, B. Acoustofluidic Measurements on Polymer-Coated Microbubbles: Primary and Secondary Bjerknes Forces. *Micromachines* **2018**, *9*, 404.

Piezoelectricity, Encyclopædia Britannica (2018), Available: https://www.britannica.com/science/piezoelectricity, (date last viewed: 01-May-19). Retrieved May 1, 2019, from https://www.britannica.com/science/piezoelectricity

The History of Ultrasound, BMUS, Available: https://www.bmus.org/about-ultrasound/history-of-ultrasound/, (date last viewed: 01-May-19). Retrieved May 1, 2019, from https://www.bmus.org/about-ultrasound/history-of-ultrasound/